

**Electrodeposition of CdTe thin films using nitrate precursor for applications in solar cells**

SALIM, H.I., PATEL, V., ABBAS, A., WALLS, J. M. and DHARMADASA, I  
<<http://orcid.org/0000-0001-7988-669X>>

Available from Sheffield Hallam University Research Archive (SHURA) at:

<https://shura.shu.ac.uk/9419/>

---

This document is the Accepted Version [AM]

**Citation:**

SALIM, H.I., PATEL, V., ABBAS, A., WALLS, J. M. and DHARMADASA, I (2015).  
Electrodeposition of CdTe thin films using nitrate precursor for applications in solar  
cells. *Journal of Materials Science: Materials in Electronics*, 26 (5), 3119-3128.  
[Article]

---

**Copyright and re-use policy**

See <http://shura.shu.ac.uk/information.html>

# Electrodeposition of CdTe thin films using nitrate precursor for applications in solar cells

H.I. Salim<sup>\*</sup>, V. Patel, A. Abbas<sup>1</sup>, M. Walls<sup>1</sup> and I.M. Dharmadasa

Electronic Materials and Sensors Group, Materials and Engineering Research Institute,  
Sheffield Hallam University, Sheffield S1 1WB, United Kingdom.

<sup>1</sup>CREST (Centre for Renewable Energy Systems and Technology), Loughborough  
University, Loughborough, Leicestershire LE11 3TU, United Kingdom.

\*E-mail: his.phys@uod.ac    Tel: +44(0) 114 225 6910    Fax: +44(0) 114 225 6930

## Abstract

Cadmium telluride (CdTe) thin films have been electrodeposited (ED) on glass/fluorine-doped tin oxide (FTO) substrates using a simplified two-electrode system in acidic and aqueous solution containing  $\text{Cd}(\text{NO}_3)_2 \cdot 4\text{H}_2\text{O}$  and  $\text{TeO}_2$ . X-ray diffraction (XRD), Optical absorption, Photoelectrochemical (PEC) cell measurements, Scanning electron microscopy (SEM) and Transmission electron microscopy (TEM) have been carried out to study the structural, optical, electrical and morphological properties of the CdTe layers respectively. The XRD study shows that the ED-CdTe layers are polycrystalline with cubic crystal structure. Results obtained from optical absorption reveal that the bandgaps of as-deposited and  $\text{CdCl}_2$ -treated CdTe layers are in the ranges  $\sim 1.50$  to  $\sim 1.54$  eV and  $\sim 1.46$  to  $\sim 1.51$  eV respectively. Observation from PEC measurements indicates p-, i- and n-type electrical conductivity for as-deposited CdTe layers grown in the cathodic voltage range (1247-1258) mV. The SEM images indicate noticeable change in CdTe grain sizes from  $\sim 85$  to  $\sim 430$  nm after  $\text{CdCl}_2$ -treatment with uniform surface coverage of the glass/FTO substrate. TEM images show the columnar growth structure for as-deposited and  $\text{CdCl}_2$ -treated CdTe layers. TEM images also indicate an increase in grain diameter from  $\sim 50$  to  $\sim 200$  nm after  $\text{CdCl}_2$ -treatment.

Keywords: Electrodeposition, CdTe, thin film, semiconductor, absorber material

## 1.0 Introduction

For several decades, enormous attention has been focused on the development of thin film semiconductors using inorganic binary compounds in order to develop low-cost and high efficiency photovoltaic thin-film solar panels. CdTe has been recognized as a suitable candidate and promising material among the group II-VI compounds to convert light into electricity due to its near-ideal direct energy band gap and high optical absorption coefficient [1, 2]. Various techniques have been used to grow CdTe thin films. These include close-space sublimation (CSS) [3], screen printing [4], sputtering [5], spray pyrolysis [6], vacuum evaporation [7] and electrodeposition (ED) [8, 9]. All these techniques have their own merits, however, electrodeposition using aqueous solution is considered to be a low-cost and energy-efficient method. In addition, simplicity, scalability and proven manufacturability are some further advantages of electrodeposition technique for manufacturing CdTe based solar panels [10-13].

It is well known that the conventional method used for the cathodic electrodeposition of CdTe thin films is the 3-electrode system which consists of a working electrode (cathode), a counter electrode (anode) and a reference electrode [14]. The need for reference electrode in 3-electrode system is due to the change of electrolyte concentration during growth process. For this reason the cathodic voltage is recorded with respect to the reference electrode. However, it should be taken into consideration that reference electrodes such as Ag/AgCl and saturated calomel, contain  $\text{Ag}^+$  and  $\text{K}^+$  which contaminate the electrolyte by acting as detrimental impurity for devices [15, 16]. These impurity ions can leak into the deposition electrolyte and drastically reduce the efficiency of fabricated solar cells based on CdTe. For this reason, in this work, simplified 2-electrode system is used instead of conventional 3-electrode system. There are various reports on the electrodeposition of thin film semiconductors using 2-electrode system which shows the reliability and applicability of this technique for fabrication of high quality thin film solar cells [17-21].

CdTe layers are usually grown using  $\text{CdSO}_4$  as the precursor for Cd ions. This paper presents the cathodic electrodeposition of CdTe thin films from acidic and aqueous solution using  $\text{Cd}(\text{NO}_3)_2$  as the precursor for Cd ions. The reports are scarce report on the electrodeposition of CdTe history, using nitrate precursor [22]. Therefore, this paper presents a comprehensive report on CdTe layers grown by 2-electrode system, using nitrate precursor in order to investigate its suitability for use in electronic devices.

## 2.0 Experimental Details

The initial Cd-precursor was prepared by dissolving 1.0M  $\text{Cd}(\text{NO}_3)_2 \cdot 4\text{H}_2\text{O}$  of 99.0% purity in 800 ml of deionized water. Then, the prepared solution was electro-purified by applying a cathodic potential just below the required potential for reduction of  $\text{Cd}^{2+}$  for  $\sim 100$  hours. The initial Te-precursor was prepared by adding 2 grams of 99.999% (5N)  $\text{TeO}_2$  powder into dilute nitric acid ( $\text{HNO}_3$ ) and continuously stirring for 24 hours. Thereafter, about 1 ml of prepared  $\text{TeO}_2$  solution was added into 800 ml aqueous solution containing purified 1.0M  $\text{Cd}(\text{NO}_3)_2 \cdot 4\text{H}_2\text{O}$ . The pH of the resulting deposition electrolyte was adjusted to  $2.00 \pm 0.02$  using either nitric acid or ammonium hydroxide ( $\text{NH}_4\text{OH}$ ) at room temperature. Both  $\text{Cd}(\text{NO}_3)_2 \cdot 4\text{H}_2\text{O}$  and  $\text{TeO}_2$  used in the deposition electrolyte were purchased from Sigma Aldrich. The substrates used for electro-purification and electrodeposition were TEC-7 glass/FTO (fluorine-doped tin oxide) with sheet resistance of  $\sim 7 \Omega/\square$  and purchased from Sigma Aldrich. Prior to electrodeposition, the glass/FTO substrates were cut into small pieces with dimensions of  $2 \times 2 \text{ cm}^2$  and washed for 15 minutes in an ultrasonic bath containing soap solution followed by rinsing with deionised water. Subsequently, the glass/FTO substrates were cleaned with methanol and rinsed with deionized water followed by a similar cleaning with acetone and deionized water. Samples were finally dried using stream of nitrogen gas. An insulating polytetrafluoroethylene (PTFE) tape was used to attach the glass/FTO substrate to a high-purity graphite rod which serves as the working electrode (cathode). Another high-purity graphite rod was used as the counter electrode (anode). The temperature of the electrolyte solution was maintained at  $\sim 85^\circ\text{C}$  with continuous moderate stirring during deposition using magnetic stirrer. The source of electrical power used for 2-electrode system was a computerised GillAC potentiostat (ACM instruments). Cyclic voltammetry was carried out to identify the approximate range of deposition potentials for CdTe at  $\sim 85^\circ\text{C}$ . The ED-CdTe layers were characterised using X-ray diffraction (XRD), Scanning electron microscopy (SEM) and Transmission electron microscopy (TEM) to study their structural and morphological properties. The electrical and optical properties of the ED-layers were characterised using photoelectrochemical (PEC) cell measurements and optical absorption. For PEC measurements, glass/FTO/CdTe and high purity graphite electrode were immersed in an electrolyte solution containing 0.1M  $\text{Na}_2\text{S}_2\text{O}_3$  to form a solid/liquid junction and the voltage across this solid/liquid interface was measured using a digital voltmeter. The voltages were recorded under dark and illuminated conditions, and the difference between these two voltages represents the PEC signal.

### 3.0 Results and Discussion

#### 3.1 Cyclic Voltammogram

Cyclic voltammograms were recorded for three separate deposition electrolytes at  $\sim 85^\circ\text{C}$  in order to study the deposition mechanism of Cd and Te to form CdTe. The first electrolyte contained 1 ml of  $\text{TeO}_2$  solution diluted in 800 ml of deionised water. The second electrolyte contained 1.0M  $\text{Cd}(\text{NO}_3)_2 \cdot 4\text{H}_2\text{O}$  in 800 ml of deionised water and the third electrolyte contained a combination of above two solutions in 800 ml of deionised water. The respective voltammograms are shown in figures 1, 2 and 3. For all three separate solutions, the same deposition conditions were used prior to recording of the voltammograms. The pH of each solution was adjusted to  $2.00 \pm 0.02$ , the temperature was maintained at  $\sim 85^\circ\text{C}$  and cyclic voltammograms were recorded at a sweep rate of  $3 \text{ mVs}^{-1}$  in the cathodic voltage ranges of (0-2000) mV in each case.

As shown in Fig. 1, during the forward cycle, as the cathodic potential is increased, the deposition of Te takes place from the  $\text{TeO}_2$  solution. The enlargement of point A (inset) shows that Te deposition starts from 196 mV according to the following electro-chemical reaction:



With gradual increase in cathodic potential the cathodic current also increases through the electrolyte. This indicates that more energy is available for Te to be deposited on the cathode surface. Noticeable increase in cathodic current at the hump 1 of the forward cycle indicates the occurrence of second electro-chemical reaction at cathodic potential of  $\sim 990 \text{ mV}$  as follow:



This reaction at higher voltages leads to dissolution of Te from the cathode forming  $\text{H}_2\text{Te}$ . Therefore, at the higher voltages deposition of Te layers can reach a saturation point without increasing the thickness of Te layer.

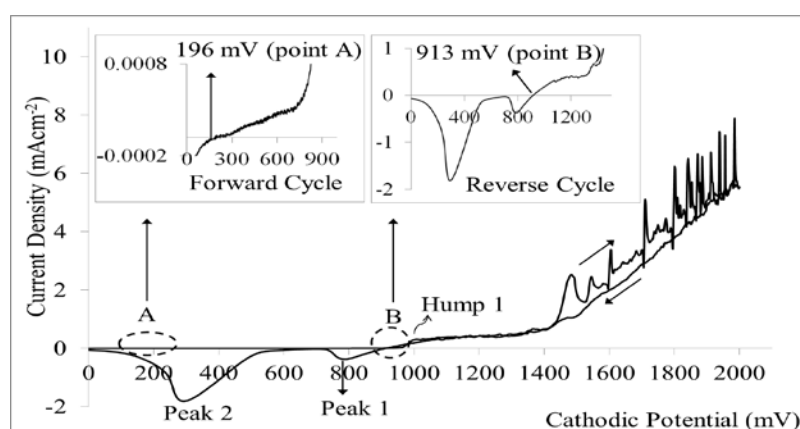
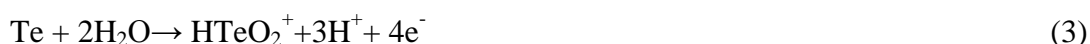


**Fig. 1.** A typical cyclic voltammogram of 800 ml deposition electrolyte containing 1 ml  $\text{TeO}_2$  solution. Note that for deposition electrolytes the pH was adjusted to  $2.00 \pm 0.02$  at room temperature, and deposition temperature was kept at  $\sim 85^\circ\text{C}$ . The insets are expansions of the points labelled A, B.

Cathodic current remains approximately steady between  $\sim 1000$  to  $\sim 1400$  mV. Beyond  $\sim 1400$  mV, rapid increase in cathodic current represents the occurrence of hydrogen evolution or electrolysis of water as it is well known that the minimum standard potential required for electrolysis of water is about 1.23 V [23]. The current peaks with varying height show formation of  $H_2$  bubbles on the cathode and subsequent release from the surface.

In the reverse cycle, when the cathodic potential decreases, the dissolution rate of Te increases in addition to deposition of Te. The appearance of anodic peak 1 at  $\sim 791$  mV and anodic peak 2 at  $\sim 292$  mV respectively represent the dissolution of elemental Te and Te bonded to the FTO-surface. The electro-chemical reaction for anodic peak 2 can be written as:



A similar scenario can be seen in Fig. 2 for  $\text{Cd}(\text{NO}_3)_2$  solution. As the cathodic potential starts to increase in forward cycle, the  $\text{Cd}^{2+}$  discharges depositing Cd on the cathode. The discharge rate of  $\text{Cd}^{2+}$  on the cathode surface increases towards higher cathodic potentials and appears as small hump 2 at  $\sim 1000$  mV which represent the following chemical reaction:



In the reverse cycle, with decrease in cathodic potential the dissolution rate of Cd also increases. The dissolution rate is small at peak 3 ( $\sim 1395$  mV) and reaches its maximum value at peak 4 ( $\sim 1271$  mV). Peak 3 and peak 4 respectively represent the dissolution of elemental Cd and Cd bonded to the FTO-surface. The electro-chemical reaction for anodic peak 3 can be written as follows:

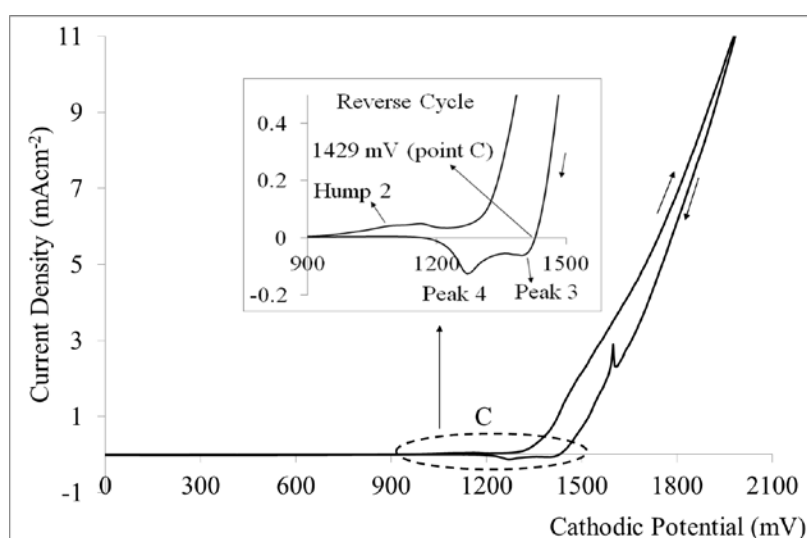


**Fig. 2.** A typical cyclic voltammogram of 800 ml deposition electrolyte containing 1.0M  $\text{Cd}(\text{NO}_3)_2 \cdot 4\text{H}_2\text{O}$ . Note that for deposition electrolytes the pH was adjusted to  $2.00 \pm 0.02$  at room temperature, and deposition temperature was kept at  $\sim 85^\circ\text{C}$ . The inset is the expansion of the area labelled C.

By comparison between figures 1 and 2, and referring to the standard reduction potential table, Te with  $E^{\circ} = +593$  mV is a more noble chalcogen and has a more positive reduction potential in comparison to Cd with  $E^{\circ} = -403$  mV ( $E^{\circ}_{\text{Te}} > E^{\circ}_{\text{Cd}}$ ) [24], and hence, Te will be deposited first on the substrate as shown in Eq.1. The quantity  $E^{\circ}$  here represents the standard reduction potential for any element versus saturated hydrogen electrode (SHE) as given in the Nernst equation.

Fig. 3 shows the voltammogram recorded for the combined solution containing both  $\text{Cd}(\text{NO}_3)_2 \cdot 4\text{H}_2\text{O}$  and 1 ml of  $\text{TeO}_2$ . In this case, point D in Fig. 3 indicates that the deposition of Te on the cathode starts at 147 mV. As the cathodic potential increases gradually, at  $\sim 1100$  mV hump 3 appears. Here, hump 3 represents the deposition of Cd on the cathode which previously was shown in Eq. (4). The cathodic current remains steady between  $\sim 1200$  to  $\sim 1400$  mV. Thus, the co-deposition of CdTe thin film is taking place in this voltage range which agrees with experimental observation. At cathodic potentials more than  $\sim 1400$  mV, cathodic current increases rapidly which can be either due to Cd dendrites formation or the generation of hydrogen gas (electrolysis of water). Although the generation of hydrogen gas at the cathode surface can be helpful in passivating defects, it can reduce the adhesion of CdTe layers to the glass/FTO substrate [13]. The overall reduction reaction for formation of CdTe thin film can be obtained from combination of Eq. (1) and Eq. (4) as follows:



In the reverse cycle of Fig. 3, with the decrease in cathodic potentials, zero current was observed at  $\sim 833$  mV (point E). At point (E), the rate of deposition and dissolution are equal. After point E, the dissolution rate reaches to its maximum values at anodic peak 5 ( $\sim 633$  mV) and anodic peak 6 ( $\sim 326$  mV). The two anodic peaks 5 and 6 respectively represent the dissolution of elemental Cd and Cd bonded to the CdTe layer, and finally Te from the cathode.

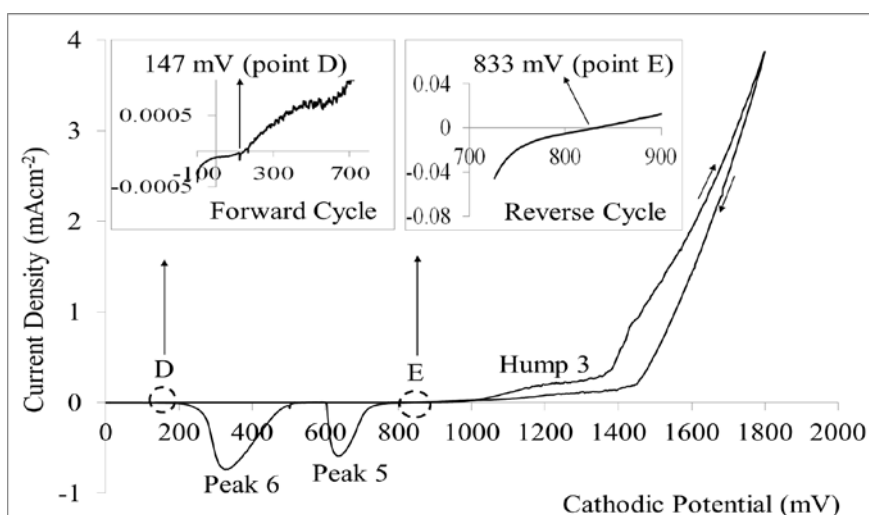


**Fig. 3.** A typical cyclic voltammogram for electrolyte containing the combination of 1.0M  $\text{Cd}(\text{NO}_3)_2 \cdot 4\text{H}_2\text{O}$  and 1 ml  $\text{TeO}_2$ . Note that for deposition electrolytes the pH was adjusted to  $2.00 \pm 0.02$  at room temperature, and deposition temperature was kept at  $\sim 85^\circ\text{C}$ . In each case, the insets are expansions of the points labelled D and E.

By comparison between figures 1, 2 and 3, it can be shown that in Fig. 3 the anodic peaks and cathodic humps of the CdTe voltammogram shift toward the more positive reduction potential values in comparison to those of Cd and Te alone. This indicates that the heat of formation of CdTe is released easing the formation of CdTe. In the electrodeposition of CdTe thin film it is important to maintain the deposition of CdTe thin films close to stoichiometry. For this reason, usually the concentration of  $\text{Cd}^{2+}$  ions is kept higher than that of the chalcogen, Te [14]. In this work, the aim in using low pH value is to prevent the formation of cadmium hydroxide phases and to increase the solubility of Te in the deposition electrolyte.

### 3.2 Photoelectrochemical (PEC) cell Analysis

PEC measurements were carried out to determine the electrical conductivity types of ED-CdTe layers. This method relies on the potential barrier formation at the solid/liquid interface between CdTe and a suitable electrolyte by immersing glass/FTO/CdTe into the electrolyte solution containing 0.1M  $\text{Na}_2\text{S}_2\text{O}_3$ . In PEC cell, the difference between the voltages under dark and illumination conditions represents the PEC signal or the open circuit voltage of the solid/liquid junction. Depending on the conductivity type of the CdTe layers, the band bending in the solid/liquid interface is different and electrons can move away or towards the solid/liquid interface. The sign of the PEC signal indicates the electrical conductivity type of the CdTe layers provided the PEC system is properly calibrated using semiconductors with known conductivity types. When the PEC signal is positive in the PEC system used, the electrical conductivity is p-type, otherwise, negative PEC signal indicates n-type electrical conductivity. Both metals and insulators show zero PEC signal due to the very narrow depletion region in the case of metals and very wide depletion region in the case of insulators. In addition, zero PEC signal can represent an intrinsic semiconductor. The magnitude of the PEC signal gives some qualitative information about doping density and strength of the depletion region [13]. In electrodeposition technique, due to deposition of CdTe layers on conducting glass/FTO substrate, it is not possible to use the more comprehensive conductivity type measurements such as Hall Effect due to underlying conducting FTO layer. For this reason, simple PEC cell was used to determine the electrical conductivity type of electrodeposited layers.

In this work PEC measurements were carried out on CdTe layers grown at cathodic potential ranges of 1200 to 1600 mV in order to identify the Te-rich, stoichiometric and Cd-rich CdTe growth voltages. For this reason CdTe layers were grown on glass/FTO substrate for a period of two hours. Each glass/FTO/CdTe was divided into two parts; first part remains as-deposited and the second part annealed at 390°C with  $\text{CdCl}_2$  for 10 minutes in air, and the results are presented in Tables 1, 2 and figures 4a and 4b. Experimental observation reveals two deposition regions for as-deposited CdTe thin films. The first region reveals the Te-rich region starting from 1200 to 1252 mV with positive PEC signals. In this region, because the CdTe layers are rich in Te, the expected electrical conduction type is p-type as experimentally observed. The values of the positive PEC signals gradually reduce from  $V_g=1200$  mV toward 1252 mV. At the cathodic potential of 1253 mV zero PEC signal was observed which represents the stoichiometric point (see figures 4a and 4b). The second region shows the Cd-rich region starting from 1254 to ~1600 mV with negative PEC signal. Since

the CdTe layers are rich in Cd, the expected electrical conduction type is n-type. In this region from 1254 to ~1450 mV the value of negative PEC signal increases. After ~1450 mV, negative PEC signal reduces due to  $n^+$  doping as a result of higher amounts of metallic Cd incorporated in the CdTe layer (see Fig. 4a). This is one of the strengths of electrodeposition technique which shows that by simply changing the growth voltage, p-, i- and n-type CdTe can be grown without addition of external impurities [12]. Doping in this case is by changing the composition of the semiconductor elements in ppm level.

**Table 1:** PEC signals of as-deposited and CdCl<sub>2</sub>-treated CdTe samples grown at cathodic potentials from 1200 to 1600 mV.

Cathodic Potential (mV)	PEC Signal (mV)	
	As-deposited	CdCl <sub>2</sub> - treated
1200	+75	+31
1225	+55	+22
1235	+54	+31
1275	-90	+41
1300	-102	-82
1350	-83	+13
1375	-94	+31
1400	-138	-14
1425	-148	-61
1450	-194	-114
1510	-51	-7
1520	-13	+20
1530	-73	-52
1540	-122	-35
1550	-56	+68
1570	-102	+32
1580	-10	+38
1590	-49	-21
1600	-97	-11

The results shown in Fig. 4b clearly show that when CdTe is Te-rich and p-type, the layers move towards n-CdTe when heat-treated with CdCl<sub>2</sub>. Therefore, the Cd-deficiency must play an important role in this change of doping concentration. When the layers are grown close to the inversion voltage ( $V_i$ ), the type conversion can go in either direction; n towards p or p towards n depending on the initial and final defects distributions [25, 26]. In this particular set of samples i-layer has become n-type after CdCl<sub>2</sub>-treatment. When initial CdTe layers are Cd-rich, and n-type, CdCl<sub>2</sub>-treatment changes the doping concentration to make the layers move towards p-type conduction. Therefore, the Te-deficiency must play an important role in this change of doping concentration. These results therefore reveal that the change from one conductivity type towards another, after CdCl<sub>2</sub>-treatment, depends on the material's initial electrical conduction type, heat-treatment temperature and duration of annealing.

**Table 2:** PEC signals of as-deposited and CdCl<sub>2</sub>-treated CdTe samples grown at cathodic potentials from 1247 to 1258 mV.

Cathodic Potential (mV)	PEC Signal (mV)	
	As-deposited	CdCl <sub>2</sub> -treated
1247	+54	+31
1248	+51	-16
1249	+47	+7
1250	+37	-120
1251	+24	-195
1252	+23	-39
1253	0	-49
1254	-28	+18
1255	-34	+5
1256	-52	-20
1257	-63	+20
1258	-78	+17

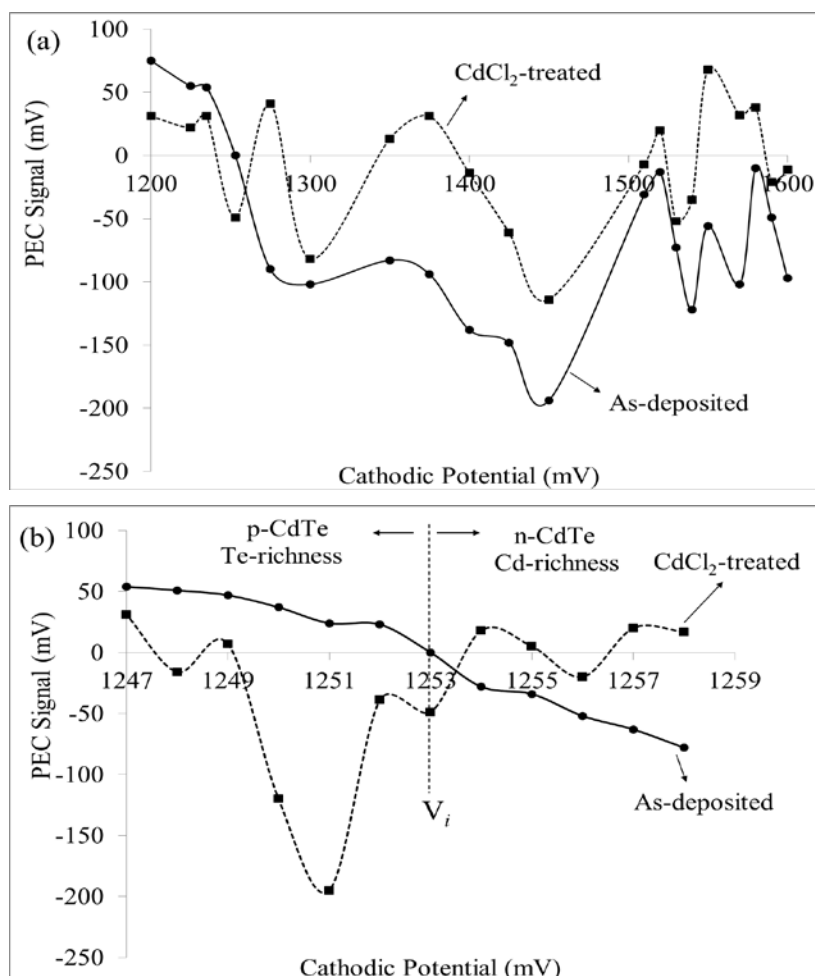


**Fig. 4.** PEC signal of the as-deposited and CdCl<sub>2</sub>-treated samples grown at cathodic potentials of (a) 1200 to 1600 mV and (b) 1247 to 1258 mV.

### 3.3 X-ray Diffraction

X-ray diffraction (XRD) was carried out using Philips PW 3710 X'pert diffractometer with Cu-K $\alpha$  monochromator of wavelength  $\lambda=1.5416$  Å. The X-ray generator tension and current were adjusted to 40 kV and 40 mA respectively. The XRD was carried out to identify the phases, crystal structure and degree of crystallinity of the ED-CdTe layers grown on glass/FTO substrates.

In this work, the aim was to determine the growth voltage corresponding to stoichiometric CdTe layers, by observing the most intense XRD peak, within the cathodic potentials ranges of (1249-1257) mV. For this reason, CdTe layers were grown at different cathodic voltages from (1249-1257) mV and then layers were annealed with CdCl $_2$ -treatment. Then, the XRD patterns of the as-deposited and CdCl $_2$ -treated CdTe layers were plotted against angle ( $2\theta$ ) and results are shown in figures 5a and 5b respectively. In this work, all as-deposited and CdCl $_2$ -treated CdTe layers were shown to be polycrystalline with cubic crystal structure and strongly oriented along (111) plane. However, CdTe can be found in hexagonal crystal structures form [27]. In this reports, the most intense XRD peak was observed at cathodic potential of 1253 mV for as-deposited CdTe layer when XRD peak intensities were plotted against growth voltages (see Fig. 6).

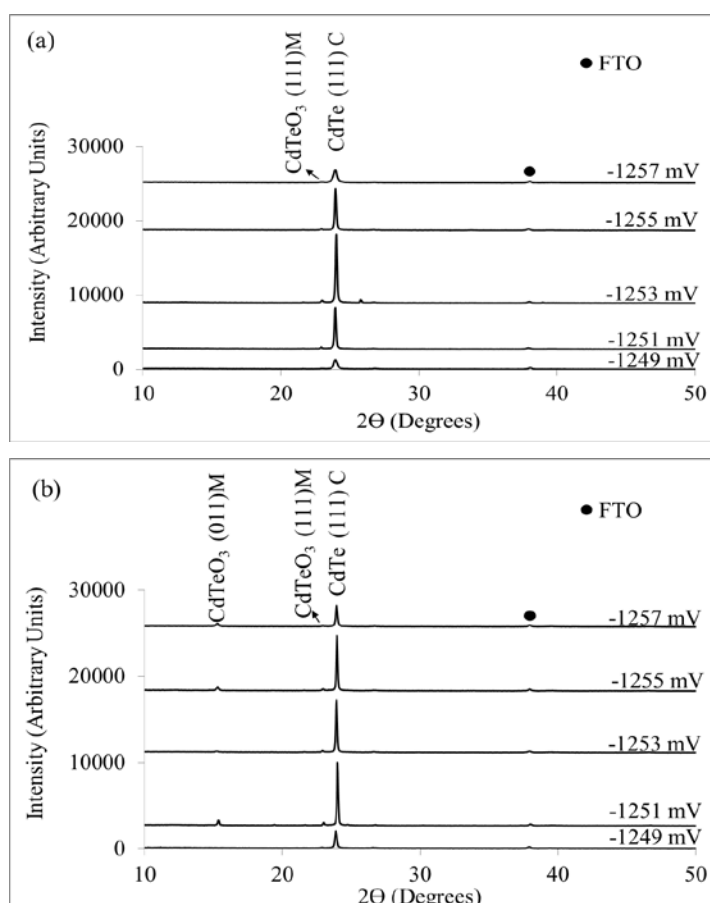


**Fig. 5.** XRD patterns of CdTe layers grown at cathodic voltage range of 1249 to 1257 mV (a) for as-deposited and (b) for annealed with CdCl $_2$ -treatment. Note that the growth duration for all layers was 2 hours.

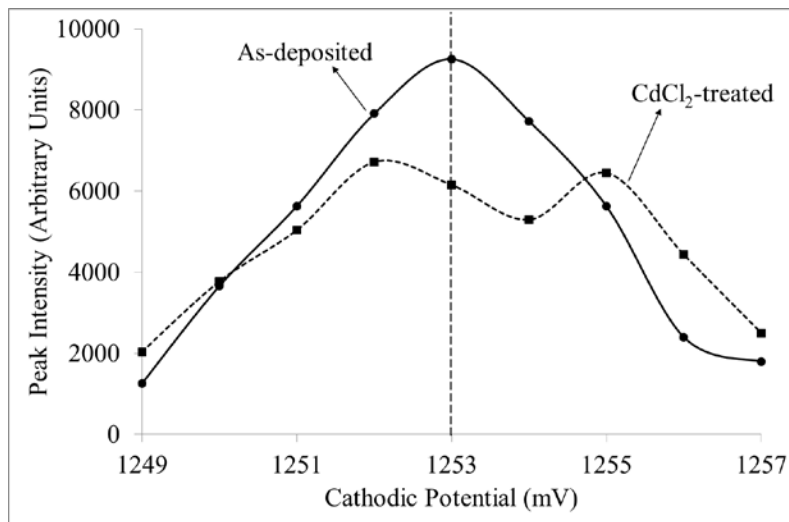


**Fig. 6.** XRD (111) peak intensity against cathodic potential for as-deposited and CdCl<sub>2</sub>-treated CdTe layers. Note that the growth duration for all layers was 2 hours.

Therefore, in order to identify all phases and crystal structures, XRD peaks analysis is mainly focused on the as-deposited CdTe layer grown at cathodic voltage of 1253 mV and then results were compared with the same sample after CdCl<sub>2</sub>-treatment as shown in Fig. 7 and Table 3. In Fig. 7, the peak intensity is plotted using log-scale against angle ( $2\theta$ ) aiming for better identification of all XRD peaks. Again, the preferentially orientation of cubic (111) plane can be clearly seen for both as-deposited and CdCl<sub>2</sub>-treated CdTe layers shown in Fig. 7. The fluctuation in XRD peak intensities were observed after CdCl<sub>2</sub>-treatment at 390°C for 10 minutes in air. The CdTe (111), CdTe (220) and CdTeO<sub>3</sub> (111) peak intensities slightly reduced and slight increase in CdTe (311) peak intensity was observed. An additional peak observation at  $2\theta = 15.25^\circ$  after CdCl<sub>2</sub>-treatment represents the reflection from a monoclinic CdTeO<sub>3</sub> (011) plane. The change in XRD peak intensities and observation of new peak can be attributed to the re-orientation of the grains of CdTe layers after CdCl<sub>2</sub>-treatment in the presence of oxygen.

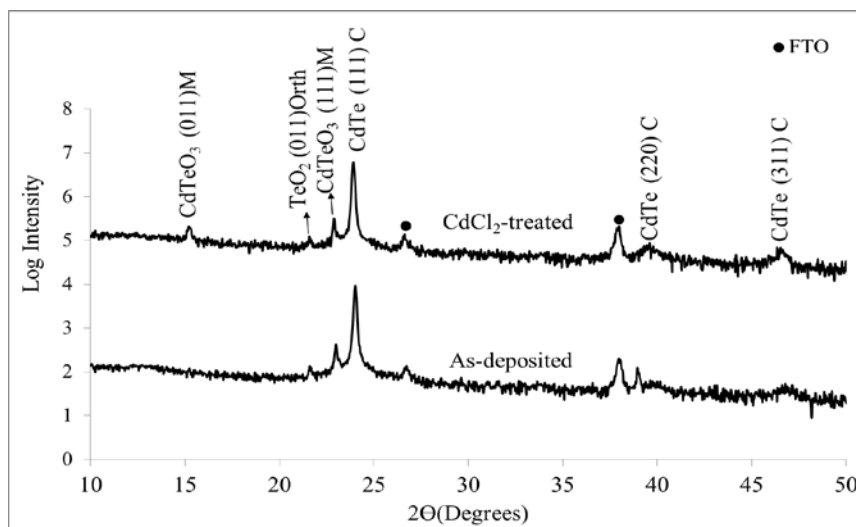


**Fig. 7.** XRD patterns of as-deposited and CdCl<sub>2</sub>-treated CdTe layer grown at 1253 mV plotted in semi-log scale. Note that the growth duration for the layer was 2 hours.

**Table 3:** XRD analysis of as-deposited and CdCl<sub>2</sub>-treated CdTe layers grown at cathodic potential of 1253 mV for 2 hours.

Sample	2θ°		Lattice Spacing D (Å)		(hkl)	Chemical Formula /Phase
	OB	RP	OB	RP		
AD-CdTe	21.63	21.76	4.10	4.08	(011)	TeO <sub>2</sub> / (Orthorhombic)
	22.99	22.95	3.86	3.90	(111)	CdTeO <sub>3</sub> / (Monoclinic)
	24.01	24.02	3.70	3.70	(111)	CdTe / (Cubic)
	38.98	39.74	2.31	2.26	(220)	CdTe / (Cubic)
	46.70	46.97	1.94	1.93	(311)	CdTe / (Cubic)
CdCl <sub>2</sub> -treated CdTe	15.25	15.20	5.80	5.82	(011)	CdTeO <sub>3</sub> / (Monoclinic)
	21.62	21.76	4.10	4.08	(011)	TeO <sub>2</sub> / (Orthorhombic)
	22.90	22.95	3.88	3.90	(111)	CdTeO <sub>3</sub> / (Monoclinic)
	23.91	24.02	3.72	3.70	(111)	CdTe / (Cubic)
	39.51	39.74	2.28	2.26	(220)	CdTe / (Cubic)
	46.63	46.97	1.94	1.9326	(311)	CdTe / (Cubic)

Note: AD = As-deposited, OB = Observed from the XRD and RP = Reported in standard files (CdTe (111), (220) and (311) cubic (JCPDS 01-075-2086), CdTeO<sub>3</sub> (011) and (111) monoclinic (JCPDS 01-077-1906) and TeO<sub>2</sub> (011) orthorhombic (JCPDS 01-076-0680).

The full widths at half maximum (FWHM) and crystallite sizes were calculated for CdTe layers grown at cathodic potential ranges of 1249 to 1257 mV. These calculations were based on diffraction from CdTe (111) XRD peaks. Scherrer's equation was used to estimate crystallite sizes and results are presented in figures 8a, 8b and Table 4. These results show that, FWHM reaches their minimum values and crystallite sizes reaches to their maximum values at the voltage ranges of (1250-1255) mV. Away from these growth voltages, FWHM gradually increases and crystallite sizes gradually decreases.

The pronounced effects of CdCl<sub>2</sub>-treatment on crystallite sizes were observed at cathodic growth voltages of 1249, 1250, 1254, 1256 and 1257 mV. At other growth voltages no noticeable change in crystallite size was observed after CdCl<sub>2</sub>-treatment. However, the observation of crystallite size saturation for both as-deposited and CdCl<sub>2</sub>-treated layers can be due to the limitation in both XRD instrument and Scherrer's equation.

In this work, experimental observation showed that the most intense XRD peak was obtained at the cathodic potential of 1253 mV for as-deposited CdTe layer. Generally, the most intense XRD peaks are expected to appear close to the stoichiometric point and the deviation from the stoichiometric point results in reduce of crystallinity due to formation of CdTe layer either with Te-richness or Cd-richness. Furthermore, the presence of two phases in as-deposited and CdCl<sub>2</sub>-treated layers reduces the crystalline nature of the ED-layers. After CdCl<sub>2</sub>-treatment, XRD peak intensities can fluctuate depending on the degree of crystallisation of the CdTe layers. When CdTe is grown at 1253 mV, with the highest crystallinity, there are two effects of CdCl<sub>2</sub>-treatment; further improvement of the

crystallinity and material loss during heat treatment. In this work, The XRD intensity of (111) peak shows that material loss by sublimation dominated when the materials is grown closer to stoichiometric voltages.

**Table 4.** Variation of FWHM of the (111) XRD peak and crystallite size extracted for layers grown at different cathodic potentials for as-deposited and CdCl<sub>2</sub>-treated samples. Growth duration for each layer was 2 hours.

Cathodic Potential (mV)	FWHM (Degrees)		Crystallite size D (nm)	
	As-deposited	CdCl <sub>2</sub> -treated	As-deposited	CdCl <sub>2</sub> -treated
1249	0.259	0.194	31.2	41.72
1250	0.162	0.129	50.0	62.58
1251	0.129	0.129	62.5	62.59
1252	0.129	0.129	62.5	62.58
1253	0.129	0.129	62.5	62.58
1254	0.162	0.129	50.0	62.58
1255	0.129	0.162	62.5	50.06
1256	0.194	0.162	41.7	50.05
1257	0.259	0.162	31.2	35.76

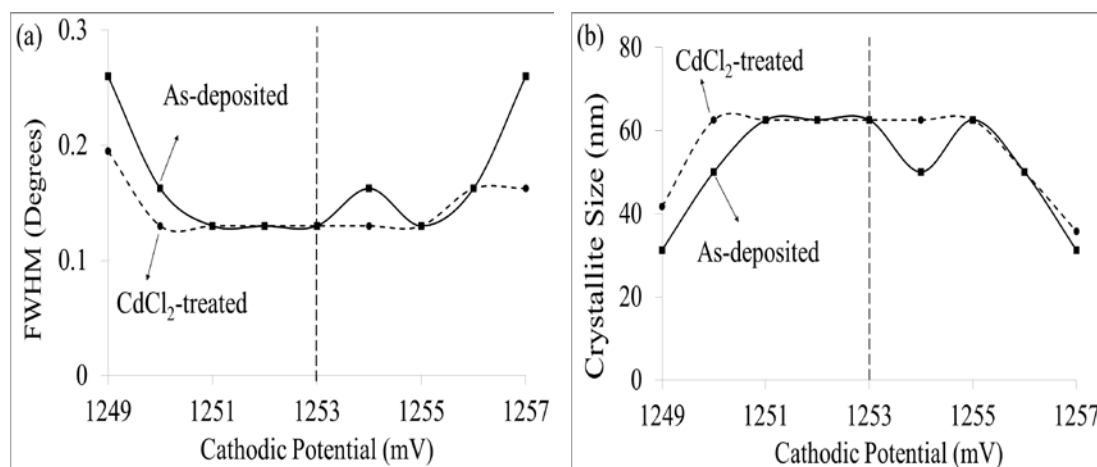


**Fig. 8.** (a) FWHM of (111) peak against cathodic potentials for as-deposited and CdCl<sub>2</sub>-treated CdTe layers grown between 1249 to 1257 mV. (b) Crystallite sizes against cathodic potentials for as-deposited and CdCl<sub>2</sub>-treated CdTe layers grown between 1249 to 1257 mV. Growth duration for all layers was 2 hours.

### 3.4 Thickness Measurements

Thickness measurements were carried out experimentally using UBM Microfocous optical depth profilometer (UBM, Messetechnik GmbH, Ettlingen, Germany). Faraday's law of electrolysis (Thickness =  $MJt/nF\rho$ ) was also used to theoretically estimate the thicknesses

where  $F = 96485 \text{ C mol}^{-1}$  is Faraday constant,  $M$  is the molar mass of the CdTe,  $\rho$  is the density of CdTe,  $J$  is the average deposition current density,  $t$  is the deposition time and  $n = 6$  is the number of electrons transferred for deposition of 1 mole of CdTe. The theoretical and experimental thickness measurements for the as-deposited CdTe layers grown at cathodic potential of 1253 mV are shown in Fig. 9. The results show that the growth duration and thickness values are directly proportional and this relationship is approximately linear. In addition, it should be taken into consideration that the theoretical thicknesses calculated from Faraday's law of electrolysis show higher values than the experimental thicknesses. This is because in Faraday's law of electrolysis, all the electronic charges are assumed to have contributed to the deposition of CdTe layers while in real case during deposition, some of the electronic charges actually participated in the electrolysis of the water especially at the cathodic voltage used (1253 mV). Hence the measured values are lower than the calculated values.

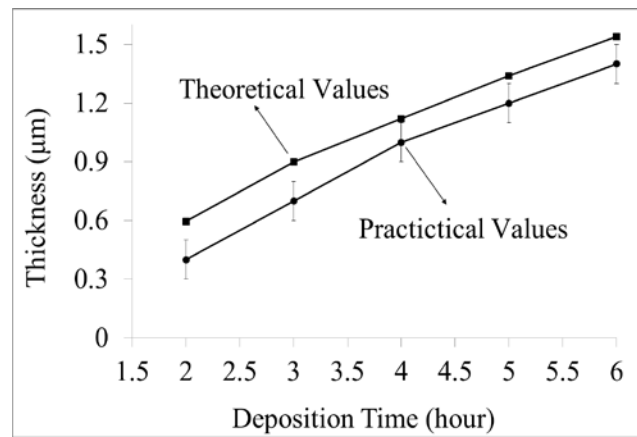


**Fig. 9.** Theoretical and experimental thickness variation with the growth time for as-deposited CdTe layers grown at cathodic voltage of 1253 mV.

### 3.5 Optical Absorption

An optical absorption measurement of the CdTe layers was carried out using Carry 50 Scan UV-VIS spectrophotometer (Varian Australia Pty. Ltd.). The CdTe layers were grown on glass/FTO substrate at growth voltage ranges of 1249 to 1257 mV for two hours duration and then samples annealed with CdCl<sub>2</sub>-treatment. The bandgap values of the as-deposited and CdCl<sub>2</sub>-treated CdTe layers were measured by plotting the square of absorbance ( $A^2$ ) versus the photon energy ( $h\nu$ ) and the results are shown in figures 10a and 10b. The results reveal that bandgap of as-deposited layers were in the range of  $\sim 1.50$  to  $\sim 1.53$  eV. After the CdCl<sub>2</sub>-treatment, slight increases in absorption with corresponding improvement in the absorption edge were observed and bandgaps shifted towards the lower energy in the range  $\sim 1.47$  to  $\sim 1.51$  eV. Slight decrease bandgap after annealing with CdCl<sub>2</sub>-treatment can be attributed to recrystallization and increase in grain sizes. Increase in absorption helps to increase the number of photo-generated charge carriers in the CdTe thin films which in turn has a positive effect on the performance of the solar cells.

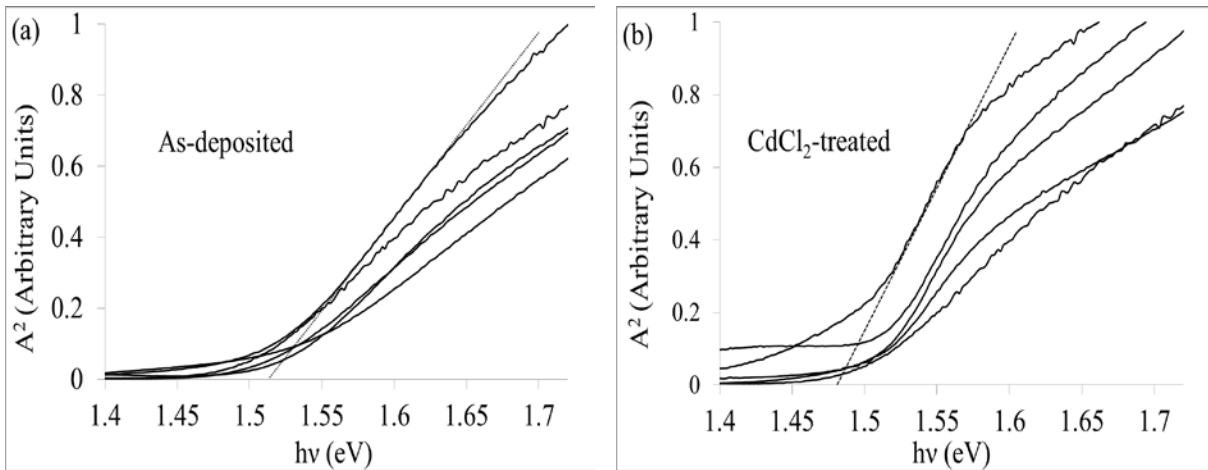


**Fig. 10.** Optical absorption spectra for (a) as-deposited and (b)  $\text{CdCl}_2$ -treated CdTe layers. The CdTe layers were grown at cathodic potential range from 1249 to 1257 mV.

Fig. 11 and Table 5 show the variation of bandgap against deposition potential for as-deposited and  $\text{CdCl}_2$ -treated layers. These results indicate that the minimum values of bandgap were observed at cathodic potential of 1253 mV for both as-deposited and  $\text{CdCl}_2$ -treated samples. Away from this growth voltage or stoichiometric point, bandgap values gradually increase. Thus, the closest experimental bandgap value to the bulk bandgap value for CdTe [28] was observed at cathodic potential of 1253 mV. Generally, bandgap values for  $\text{CdCl}_2$ -treated CdTe layer were lower than the as-deposited layers. The shift in bandgaps towards lower energy values after  $\text{CdCl}_2$ -treatment indicates that more photons are available to be efficiently absorbed for creation of photo-generated charge carriers in CdTe thin-film.

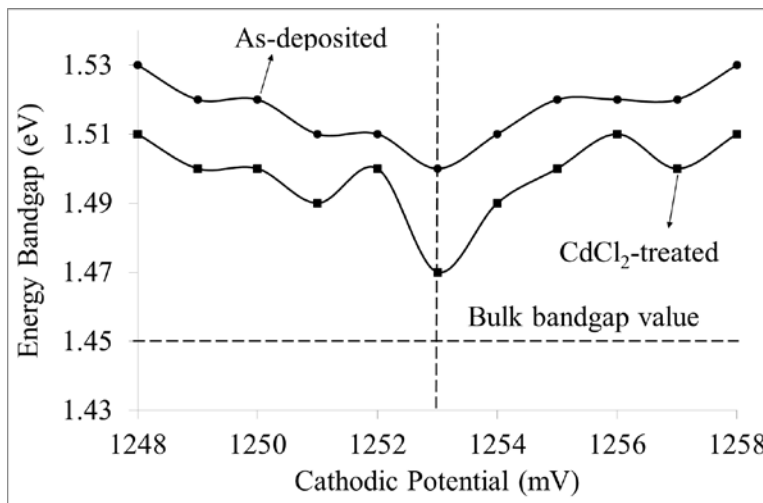


**Fig. 11.** Variation of energy bandgap with cathodic potential for as-deposited and  $\text{CdCl}_2$ -treated CdTe layers. Growth duration for all layers was 2 hours with calculated thickness of  $\sim 0.63 \mu\text{m}$ .

**Table 5.** Variation of energy bandgap with cathodic potential for as-deposited and CdCl<sub>2</sub>-treated CdTe layers. Growth duration for each layer was 2 hours.

Cathodic Potential (mV)	Energy Bandgap (eV)	
	As-deposited	CdCl <sub>2</sub> -treated
1249	1.52	1.50
1250	1.52	1.50
1251	1.51	1.49
1252	1.51	1.50
1253	1.50	1.47
1254	1.51	1.49
1255	1.52	1.50
1256	1.52	1.51
1257	1.52	1.50

In order to identify the effect of growth times and thickness of CdTe layers on the bandgap values, CdTe samples were grown at growth voltage of 1253 mV for different durations between two to six hours. Then the same samples were heat-treated with CdCl<sub>2</sub> and the results of their optical absorption measurements are shown in figures 12a and 12b. From these figures it can be seen that as the growth time increases, the absorption also increases and bandgap move towards the bulk value. This can be due to increase in thickness of CdTe layer which in turn leads to enhancement in crystallite or grain size of the CdTe layer. Here it should be noted that in electrodeposition technique it is more precise to plot the bandgap variation against the thickness rather than growth time. The reason is, during the deposition of the layer, ionic concentration and current density can change. In this case if two samples are grown for the same duration they may not end up with the same thickness. Therefore, for the as-deposited CdTe layers grown at cathodic potential of 1253 mV bandgap were preferred to be plotted against the thicknesses rather than growth time as shown in Fig. 13 and Table 6.

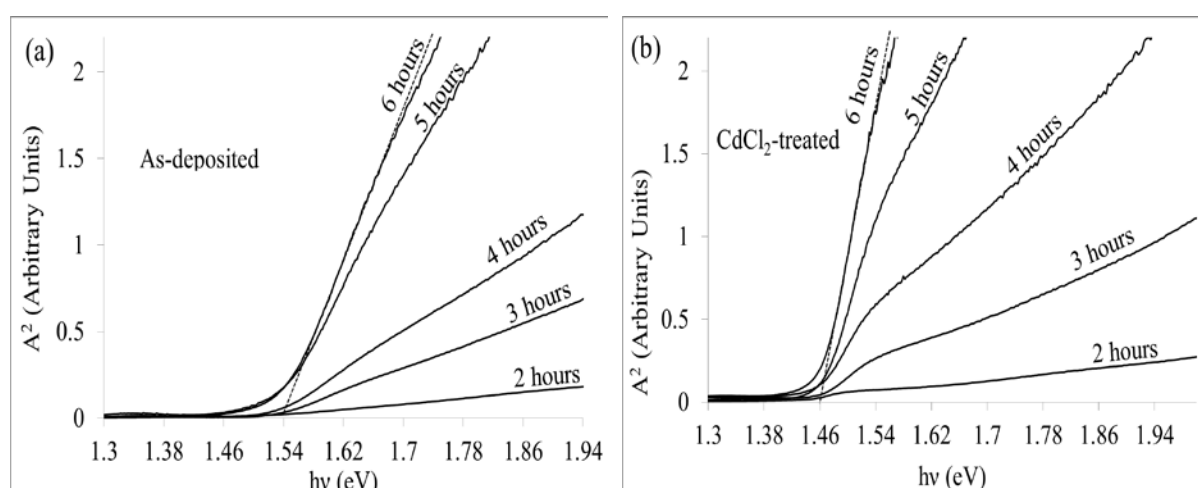


**Fig. 12.** Variation of optical absorption edge with growth time for (a) as-deposited and (b) CdCl<sub>2</sub>-treated CdTe layers. The layers were grown at cathodic potential of 1253 mV.

Results show that as the thickness of the as-deposited CdTe layer increases from  $\sim 0.60 \mu\text{m}$  to  $\sim 1.1 \mu\text{m}$  the bandgap reduces and remains steady for thickness higher than  $\sim 1.1 \mu\text{m}$ . The higher bandgap observation for lower CdTe thickness can be due to columnar growth nature of CdTe layer. Because at the early stage of the growth, CdTe layer does not completely cover the surface of glass/FTO substrate and leaves some gaps between the columnar grown materials. These transparent gaps can affect the bandgap measurements. In other words, during optical absorption measurements UV-Visible light can pass through these transparent gaps and as a result, the higher energy bandgaps will be obtained.

From Fig. 13 and Table 6 it can be clearly seen that the bandgap values of CdCl<sub>2</sub>-treated layers are less than those of as-deposited layers and are close to the bulk bandgap value. It was interesting to see that the bandgap values of CdCl<sub>2</sub>-treated samples remain unchanged ( $\sim 1.46 \text{ eV}$ ) within the thicknesses ranges of  $\sim 0.60$  to  $\sim 1.55 \mu\text{m}$ . This shows that CdCl<sub>2</sub>-treatment has the effect of reducing gaps between columnar grown CdTe due to increase in CdTe grain sizes. This observation shows that CdTe thin films with low thicknesses of about  $\sim 0.60 \mu\text{m}$  can still be used efficiently to absorb sufficient photon and in turn enhance the performance of solar cells based on CdTe.

**Table 6.** Variation of energy bandgap with growth time and thicknesses for as-deposited and CdCl<sub>2</sub>-treated CdTe layers grown at 1253 mV.

Growth Time (hours)	Thickness ( $\mu\text{m}$ )	Energy Bandgap (eV)	
		As-deposited	CdCl <sub>2</sub> -treated
2	0.59	1.54	1.46
3	0.90	1.54	1.46
4	1.12	1.53	1.46
5	1.34	1.53	1.46
6	1.54	1.53	1.46

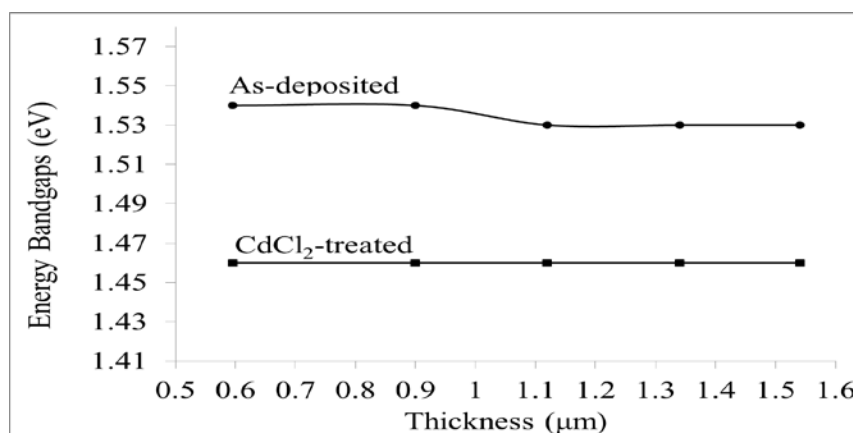


**Fig. 13.** Variation of energy bandgap with thickness for as-deposited and CdCl<sub>2</sub>-treated CdTe layers.

### 3.6 Scanning Electron Microscopy (SEM)

SEM measurement was carried out using FEI Nova 200 NanoSEM equipment on the glass/FTO/ED-CdS/ED-CdTe layer grown at 1253 mV for three hours. This sample was divided into two parts; the first part remains as-deposited, and the second part was treated with CdCl<sub>2</sub>. The SEM results are shown in figures 14a and 14b. The SEM magnification used was 60,000 for both CdTe layers. Finally, SEM cross-section was carried out on CdTe sample annealed with CdCl<sub>2</sub> with magnification of 100,000 as shown in Fig. 15. The SEM of as-deposited sample shows cauliflower-type CdTe clusters containing small grains. The gaps between clusters are visible at this magnification. The as-deposited sample contains clusters with sizes in the range of ~85 nm to ~110 nm. After CdCl<sub>2</sub>-treatment noticeable change in the cluster size is observed. This is because small clusters coalesce together and make larger clusters in the range of ~140 nm to ~430 nm. This shows that CdCl<sub>2</sub>-treatment is a necessary step for obtaining larger grains. This step will help to narrow down the gaps between grains and reduce the pinholes in the CdTe surface. In thin film solar cells, existence of gaps in the CdTe layers is detrimental due to the back metal contact reaching the front contact and therefore short-circuiting the device. Moreover, larger grains mean less scattering at grain boundaries within the CdTe and better electronic transport which can be useful in thin film solar cells.

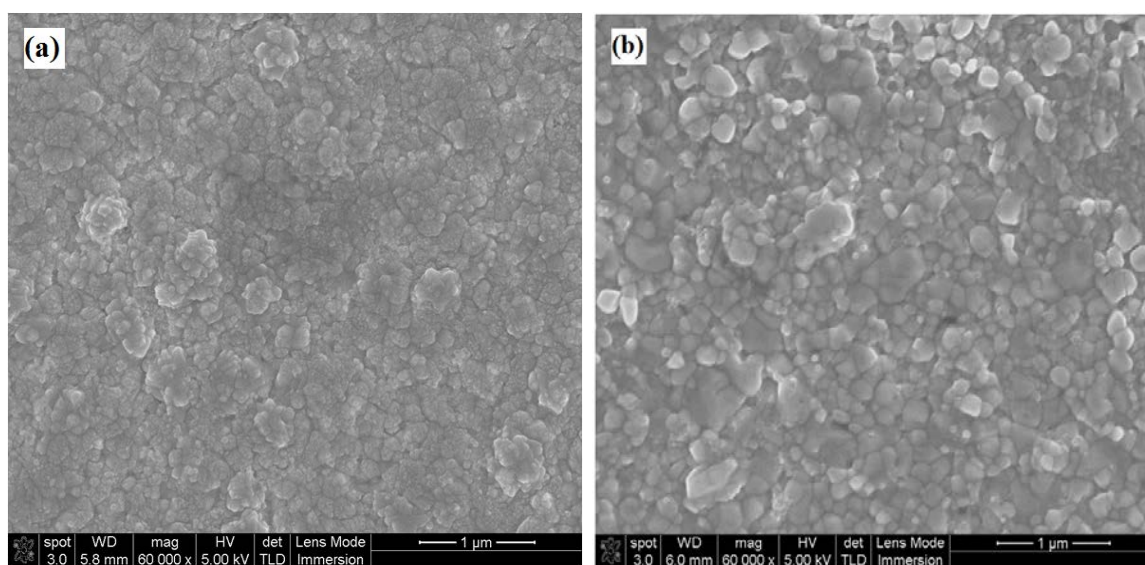


**Fig. 14.** 2D-SEM images of glass/FTO/ED-CdS/ED-CdTe layers (a) for as-deposited, (b) for CdCl<sub>2</sub>-treated samples.

The SEM cross-section taken at a magnification of 100,000 reveals that CdTe layer covers the glass/FTO/ED-CdS uniformly, with the estimated thickness of ~470 mV. However, small voids can be observed in the vicinity of FTO/CdS interface. This is because during electrodeposition the electric fields at FTO spikes is higher than those at other points and therefore nucleation starts from these spikes and the grains grow upward. This can produce non-uniformities in CdS and CdTe layers and create some gaps or voids at the glass/FTO/CdS and CdS/CdTe interfaces. The voids observed could also arise due to

incomplete cleaning of the substrate. These voids can be treated to a certain extent by annealing at a suitable temperature due to grain growth.

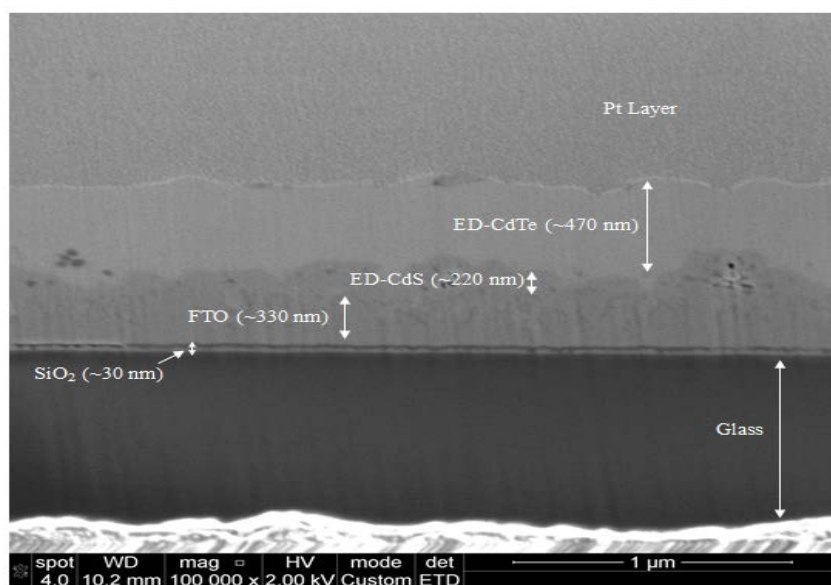


**Fig. 15.** SEM cross-section of CdCl<sub>2</sub>-treated glass/FTO/ED-CdS/ED-CdTe structure.

### 3.7 Transmission Electron Microscopy (TEM)

TEM images of the CdTe layers were taken using JEOL JEM 2000FX operating at 200 kV. Fig. 16a shows the TEM image of as-deposited CdTe layer grown at cathodic potential of 1253 mV. The estimated thickness of as-deposited CdTe layers from TEM image is ~780 nm. This image shows the columnar growth of CdTe layer with small grains in the range of ~50 nm to ~70 nm in diameter containing high density of lattice defects. The columnar and upward growth of the CdTe layer can be related to the nature of electrodeposition technique and substrate used. The nucleation of CdTe grains start from the FTO spikes where the electric field is higher than that of other points as mentioned earlier. The columnar and rough nature of glass/FTO substrate can be clearly seen in Fig. 16a. The observation of small grains in as-deposited CdTe layer can be attributed to the low-temperature growth nature of electrodeposition technique.

Fig. 16b shows the cross-section of CdCl<sub>2</sub>-treated CdTe layers. The CdCl<sub>2</sub>-treated sample shows larger grains in the range of ~70 nm to ~200 nm in diameter with columnar structure and lower defect densities. The appearance of larger grains can be related to the recrystallisation and coalescence of the smaller grains. In other words, when CdTe layer is annealed in the presence of chlorine, the crystallographic reorientation takes place and restructuring in CdTe results in an increased grain size. The observation of bright dots at Fig. 16b may be due to the voids created during sample preparation for TEM experiment.

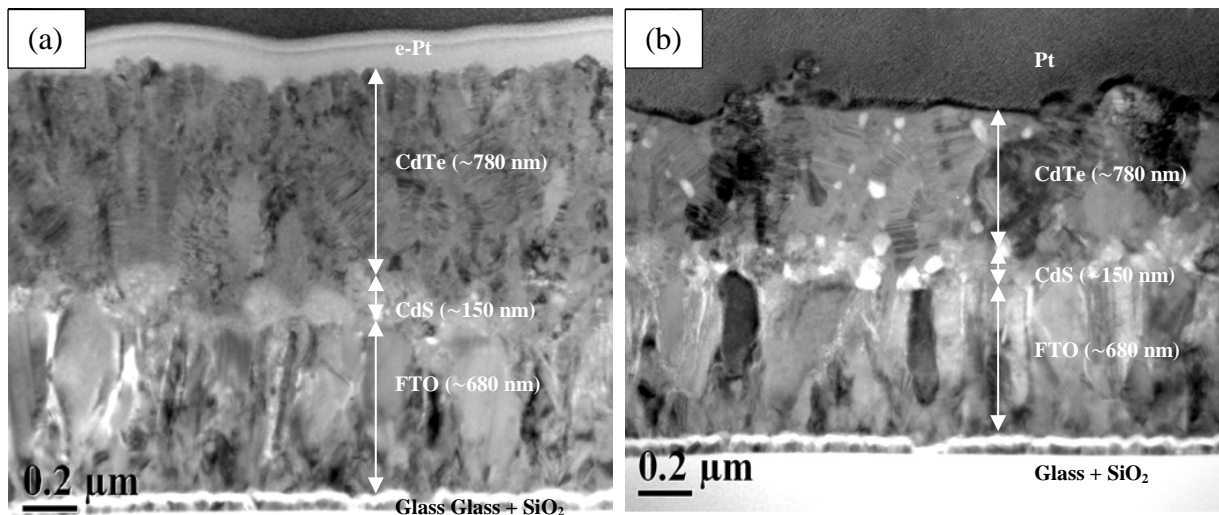


**Fig. 16.** TEM images of (a) as-deposited and (b)  $\text{CdCl}_2$ -treated CdTe layer deposited on glass/FTO/CdS substrate.

#### 4.0 Preliminary Device Results

Preliminary results of the I-V observation of solar cell structures using chemical bath deposited (CBD) CdS; glass/FTO/CBD-CdS/ED-CdTe/Au solar cell, show promising results. The I-V measurements of the preliminary solar cell were carried out under dark and illumination condition of AM 1.5 at room temperature and the results are shown in figures 17a and 17b. The initial solar cell parameters extracted from the I-V curve under illumination show open circuit voltage ( $V_{oc} = 605 \text{ mV}$ ), short circuit current density ( $J_{sc} = 25.5 \text{ mAcm}^{-2}$ ), fill factor ( $FF = 0.41$ ) and solar cell efficiency ( $\eta = 6.3\%$ ) for small device area of  $0.0314 \text{ cm}^2$  (2 mm diameter circular contacts).

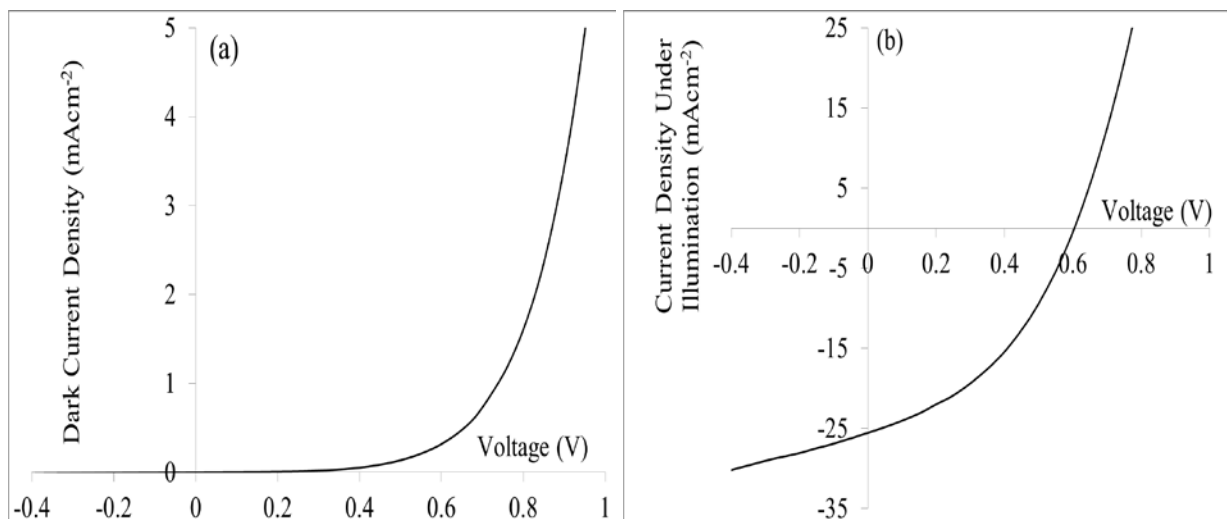


**Fig. 17.** I-V characteristics of initial glass/FTO/CBD-CdS/CdTe/Au solar cell device (a) under dark and (b) under illumination conditions.

## 5.0 Conclusion

In this work CdTe layers were successfully electrodeposited using 2-electrode system from an acidic and aqueous solution containing  $\text{Cd}(\text{NO}_3)_2 \cdot 4\text{H}_2\text{O}$  precursor. Two regions of deposition voltage for growing as-deposited p- and n-type CdTe layers were identified. The as-deposited CdTe layer was found to be stoichiometric with i-type electrical conductivity at the cathodic potential of 1253 mV. Deviation from this stoichiometric points towards Te-rich and Cd-rich regions, respectively results in p-type and n-type electrical conductivity. After  $\text{CdCl}_2$ -treatment, depending on the initial electrical conductivity type of the CdTe layer, doping concentration variations from p-type towards n-type, i-type towards n-type and n-type towards p-type have been observed. Both as-deposited and  $\text{CdCl}_2$ -treated CdTe layers strongly show (111) preferred orientation with cubic crystal structure. Bandgap values for CdTe layer were strongly affected by  $\text{CdCl}_2$ -treatment, showing the energy gap from  $\sim 1.54$  eV to  $\sim 1.46$  eV. The as-deposited and  $\text{CdCl}_2$ -treated CdTe layers show columnar structure indicating the upward CdTe grain growth during electrodeposition. Noticeable changes in CdTe grain size were observed after  $\text{CdCl}_2$ -treatment from  $\sim 110$  nm to  $\sim 430$  nm. Preliminary solar cells fabricated using this CdTe layers showed encouraging device results. Work is in progress to fully optimise the growth conditions and device processing steps toward achieving highest possible solar cell efficiencies.

## 6.0 Acknowledgement

The authors would like to thank Paul Bingham, O. K. Echendu, Fijay Fauzi, Azlian AbdulManaf, Mohammad Madugu and Olajide I. Olusola for their contributions in this work. The principal author wishes to thank the Ministry of Higher Education & Scientific Research at Kurdistan Region of Iraq for financial support.

## References:

- [1] J. J. Loferski, (Theoretical considerations governing the choice of optimum semiconductor for photovoltaic solar energy conversion), *J. Appl. Phys.*, 777, 27 (1956).
- [2] X. Wu, (High- efficiency polycrystalline CdTe thin-film solar cells), *Solar Energy*, 803-8014, 77 (2004).
- [3] T. L. Chu; S. S. Chu, C. Ferekides, C. Q. Wu, J. Britt and C. Wang, (13.4% efficient thin film CdS/CdTe solar cells), *J. Appl. Phys.* 7608, 70 (1991).
- [4] S. Ikegami. *Solar Cells*, (CdS/CdTe solar cells by the screen-printing-sintering technique: fabrication, photovoltaic properties and applications) 89-105, 23 (1988).
- [5] S. J. Sandoval, M. M. Lira, and I. H. Calderón, (Crystal structure and energy gap of CdTe thin films grown by radio frequency sputtering), *J. Appl. Phys.* 4197, 72(1992).
- [6] J. L. Boone, T. P. Van Doren and A. K. Berry, (Deposition of CdTe by spray pyrolysis). *Thin Solid Films*, 259-264, 87 (1982).

- [7] S. Lalitha, R. Sathiyamoorthy, S. Senthilarasu, A. Subbarayan, K. Natarajan, (Characterization of CdTe thin film dependence of structural and optical properties on temperature and thickness), *Solar Energy Material & Solar Cells*, 187-199, 82 (2004).
- [8] S. K. Das and G. C. Morris, (Preparation and characterisation of electrodeposited n-CdS/p-CdTe thin film solar cells), *Solar Energy Materials and Solar Cells* 305-316, 28 (1993).
- [9] B. M. Basol, (High efficiency electroplated heterojunction solar cell), *J. Appl. Phys.* 601, 55 (1984).
- [10] A. K. Turner, J.M. Woodcock, M. E. Ozsan, J. G. Summers, J. Barker, S. Binns, K. Buchanan, C. Chai, S. Dennison, R. Hart, D. Johnson, R. Marshall, S. Oktik, M. Patterson, R. Perks, S. Roberts, M. Sadeghi, J. Sherborne, J. Szubert and S. Webster, (Stable, high efficiency thin film solar cells produced by electrodeposition of cadmium telluride). *Solar Energy Materials*, 388-393, 23 (1991).
- [11] D. Cunningham, M. Rubich and D. Skinner, (Cadmium Telluride PV Module Manufacturing at BP Solar), *Prog. Photovolt: Res. Appl.*, 159-168, 10 (2002).
- [12] I. M. Dharmadasa, J. Haigh, (Strength and advantages of electrodeposition as a semiconductor growth technique for application of macroelectronic devices) *J. Electrochem. Soc.*, G47-G52, 153(1) (2006).
- [13] I. M. Dharmadasa, *Advances in thin-films solar cells*, Boulevard, Singapore, Pan Stanford, (2013) 40-44.
- [14] M. P. R. Panicker, M. Knaster and F. A. Kroger, (Cathodic Deposition of CdTe from Aqueous Electrolytes), *J. Electrochem. Soc.* 566-572, 125(1978).
- [15] S. Dennison, (dopant and impurity effects in electrodeposited CdS/CdTe thin films for photovoltaic applications), *J. Mater. Chem.*, 41-46, 4 (1994).
- [16] K. Zanio, *Semiconductors and Semimetals, Cadmium Telluride*, Academic Press, 119, 13 (1978).
- [17] I. M. Dharmadasa, R. P. Burton and M. Simmonds, (Electrodeposition of CuInSe<sub>2</sub> layers using a two-electrode system for applications for multi-layer graded bandgap solar cells), *Solar Energy Materials & Solar Cells*, 2191-2200, 90 (2006).
- [18] D. G. Diso, G. E. A. Muftah, V. Patel, and I. M. Dharmadasa. (Growth of CdS Layers to Develop All-Electrodeposited CdS/CdTe Thin-Film Solar Cells), *J. Electrochem. Soc.*, H647-H651, 157(6) (2010).
- [19] O. K. Echendu, F. Fauzi, A. R. Weerasinghi and I. M. Dharmadasa, (High short-circuit current density CdTe solar cells using all-electrodeposited semiconductors), *Thin Solid Films*, 529-534, 556 (2014).
- [20] R. N. Bhattacharya, M. K. Oh and Y. Kim, (CIGS-based solar cells prepared from electrodeposited precursor films), *Solar Energy Materials & Solar Cells*, 198-202, 98 (2012).
- [21] A. Bouraiou, M. S. Aida and E. Tomasella, (ITO substrate resistivity effect on the properties of CuInSe<sub>2</sub> deposited using two-electrode system), *J. Mater. Sci.* 1241-1244, 44 (2009).
- [22] T. Nishio, M. Takahashi, S. wada, T. Miyauchi, K. Wakita, H. Goto, S. Sato, O. Sakurada, (Preparation and Characterization of Electrodeposited In-Doped CdTe Semiconductor Films), *Electrical Engineering in Japan*, 97-102, 164 (3), 2008.

- [23] J. Sun, D. K. Zhong and D. R. Gamelin, (Composite photoanodes for Photoelectrochemical solar water splitting), *Energy Environ. Sci.*, 1252- 261, 3(2010).
- [24] P. Vanysek, *Electrochemical Series Table 1 Alphabetical*, Boca Raton: CRC Press, (2000).
- [25] B. M. Basol, (Type conversion, contacts, and surface effect on electroplated CdTe Films), *J. Appl. Phys.*, 3809-3813, 58 (1985).
- [26] S. Y. Yang, J. C. Chou and H. Y. Ueng, (Influence of electrodeposition potential and heat treatment on structural properties of CdTe films), *Thin Solid Films*, 4197- 4202, 518 (2010).
- [27] A. Luque and S. Hegedus, (*Handbook of Photovoltaic Science and Engineering*), John Wiley & Sons, Ltd., 623-624 (2003).
- [28] T. L. Chu and S. S. Chu, (Thin Film II-VI Photovoltaics), *Solid-State Electronics*, Vol. 533-549, 38 (3) (1995).